Raman study of the oxygen anharmonicity in $YBa_2Cu_3O_x$ ($6.4<x<7.0$) superconductors

D. Palles, N. Poulakis, and E. Liarokapis
Physics Department, National Technical University, Athens 157 80, Greece

K. Conder and E. Kaldis
Laboratorium für Festkörperphysik, Edgenössische Technische Hochschule Honggerberg, CH-8093 Zürich, Switzerland

K. A. Müller
IBM Zürich Research Lab. Saumerstr. 4, CH-8803 Rüschlikon, Switzerland

(Received 29 February 1996)

A systematic Raman study in the visible and the near IR has been carried out on $YBa_2Cu_3O_x$ samples, with isotopic substitution of ^{18}O for ^{16}O, and for oxygen concentrations in the range $x=6.44-6.98$. A small but clear deviation from harmonic behavior has been detected for the frequency shift of the in-phase mode and, to a less extent, of the apex mode, relative to the out-of-phase phonon. The deviation increases towards low concentrations of oxygen. A disagreement of the present work for the apical mode, with a previous investigation using IR excitation, is attributed to the contribution of several phases to the apex mode in the underdoped region and the possible IR resonance of the ''ortho-II'' phase. [S0163-1829(96)07733-8]

I. INTRODUCTION

A possible explanation of the small oxygen isotope effect observed in the ceramic superconductors, within the frame of the phonon-mediated pair-coupling mechanism, is based on the enhancement of the electron-phonon coupling strength through the anharmonic motion of the oxygen atoms.[1–5] In this scheme the strong electron-phonon coupling results from a multiple well potential in the motion of the oxygen atoms.[5] Among the different oxygen sites which are encountered in these superconductors, the apex oxygen has been observed to be in anharmonic potential.[6,7] In recent years, a systematic research of the oxygen diffusion mechanisms at the various oxygen atomic sites resulted in a controllable way of oxygen isotopic substitution for the 123 compounds.[8] On such specially prepared compounds the possibility of an anharmonic potential for the apex oxygen or the other oxygen atoms has been investigated using Raman spectroscopy.[9] It has been discovered that, among the three different sites occupied by oxygen, the out-of-phase vibrations of the oxygens at the planes (O2,3) do not show any anharmonic dependence in the whole range of oxygen concentration studied, while the apex oxygen presents a characteristic deviation from the harmonic approximation which seemed to be beyond the experimental error.[9] On the other hand, the anharmonicity observed in Ref. 9 seems to be roughly independent of the oxygen concentration. A similar anharmonic effect has been observed by others,[10] but it has been attributed to the different amount of isotopic substitution at each of the oxygen sites. Indications for anharmonicity were found also by other investigators.[11,12]

In this work a systematic Raman study has been carried out, using two series of carefully synthesized and characterized samples $YBa_2Cu_3{}^{16}O_x$ and $YBa_2Cu_3{}^{18}O_x$ with ^{18}O substituted in the range 85–90 % for ^{16}O. In both cases the oxygen concentration was varied in the range 6.4–6.98.

II. SYNTHESIS OF THE SAMPLES

In view of the structural and chemical complexities of $YBa_2Cu_3O_x$ and their influence on its physical properties, it is very important to have very carefully synthesized and characterized materials. Details about the sample preparation for the ^{16}O samples have been given elsewhere.[13] The isotope exchange with ^{18}O was performed in sealed ampoules at 450 °C for 100 h. This temperature has been found optimal as a result of a thermodynamic study of the isotope exchange.[8] However, this much lower temperature of annealing and the complexity of the isotope exchange do not allow as high a homogeneity for the ^{18}O series as that of the ^{16}O series. Isotope gas from ISOTEC France containing 96.5% of $^{18}O_2$ (the rest were both ^{17}O and ^{16}O isotopes) was used. The $^{18}O_2$ gas in the ampoule was changed many times so that an isotope content in the sample up to 90% could be obtained. The isotope content in the samples was determined using thermogravimetry and recording the weight change after a reexchange of the ''heavy'' isotope ^{18}O, by heating the sample in a stream of ^{16}O.

Using the volumetric method discussed in the past,[14] the oxygen content could be determined with an accuracy of $\Delta x=\pm 0.001$ in the oxygen stoichiometry coefficient of the orthorhombic samples. We note, however, that this very high accuracy is possible only for phase pure samples. An impurity phase of 1% wt. would increase the error up to $\Delta x=0.005$.

The phase purity of the samples was examined with a STOE powder diffractometer. No other phases apart from 123 were found. The sensitivity of the instrument for impurity phases was determined to 0.5 wt. %, using a calibration with standards containing different amounts of $BaCuO_2$, which is the most common impurity in 123. Besides, the Raman investigations have not shown any evidence of this phase.

III. EXPERIMENT

A total number of 38 samples (19 with ^{16}O and 19 with ^{18}O) have been measured in this work. The Raman spectra were obtained with a T64000 Jobin-Yvon triple spectrometer, equipped with a liquid-nitrogen-cooled CCD and a microscope. The 514.5, 488.0, 647.1, and 752.5 nm lines of Ar^+ and Kr^+ lasers were used for excitation, at low power which was kept fixed during the measurements at the level of 0.1–0.5 mW, depending on the laser wavelength. The spectra were measured on microcrystallites (platelets) and by employing a polarizer and an analyzer the scattering configurations $y(zz)\bar{y}$ and $y(xx)\bar{y}$ or $x(yy)\bar{x}$ were selected, where the z axis coincides with the c axis and the x and y axes are located in the a-b plane of the microcrystallites. The proper orientation of the microcrystallites was selected from their shapes and from the scattering selection rules of the $4A_g$ and B_{1g} phonons. The spectra have been calibrated using some low-frequency plasma lines or a silicon wafer used as a reference, and when necessary they have been corrected accordingly. The possibility of a local heating of the samples by the applied laser beam was excluded by studying the spectra on various power densities.

Accumulation times were of the order of 1–1.5 h for the green and the blue lines but 4–5 h for the 752.5 nm line, due to the small cross section. A number of microcrystallites (varying from 7 to 10 for the visible and 1–3 for the NIR) were studied for each oxygen concentration, for better statistics. Most measurements were performed at room temperature, but some samples have also been measured at liquid-nitrogen temperature. Any statistical fluctuations observed in the phonon frequencies from different microcrystallites can be attributed either to surface effects of the crystallites or to an inhomogeneous distribution of oxygen inside the samples. The possibility of a variation in the oxygen distribution among the different microcrystallites or inside each one (the laser beam probes only a 100 nm layer from the surface) cannot be excluded, but it is expected to be minimized from the preparation conditions.

IV. LOW-FREQUENCY AND NEW MODES

Typical spectra for selected dopings are presented in Figs. 1(a), 1(b), 2(a), and 2(b) for both $y(zz)\bar{y}$ and $y(xx)\bar{y}$ polarizations and for the two oxygen isotopes. Except from the overall shift in frequency of the oxygen modes due to the isotopic substitution, the two sets of spectra look quite similar. Characteristic changes are observed in the frequency of both the apex (O4) oxygen as the oxygen content decreases below 6.7, and the in-phase vibrations of the plane oxygens (O2,3), which decreases continuously with doping. On the other hand, the out-of-phase phonon of the plane oxygens of B_{1g} symmetry is only slightly affected by the amount of oxygen (Figs. 1 and 2).

For the low-frequency modes, the variation with oxygen concentration x of their frequencies is presented in Figs. 3 and 4 for ^{16}O and ^{18}O, respectively. No difference is observed between the two isotope series regarding the Ba phonon at $\sim$116 cm^{-1} and the Cu2 phonon at $\sim$150 cm^{-1} which proves the negligible amount of coupling between the motion of the oxygen atoms and the vibrations of the Ba, Cu2 atoms. In the zz polarization [Figs. 1(a) and 2(a)] the relative

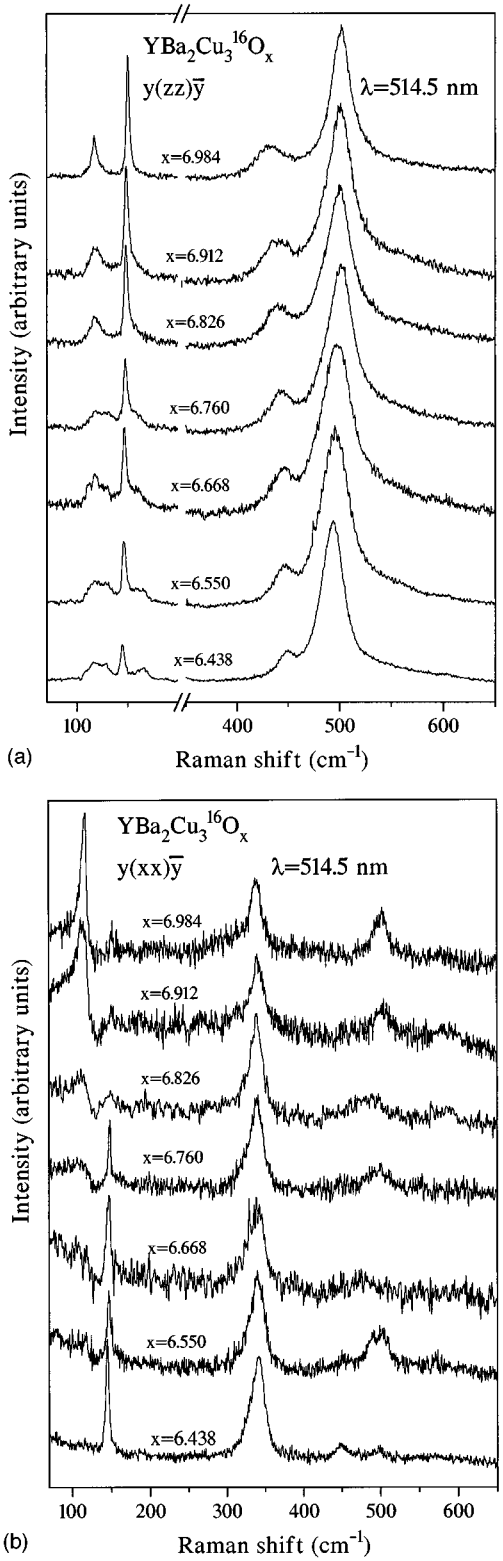

FIG. 1. Raman spectra for selected oxygen concentrations for the ^{16}O samples and for the $y(zz)\bar{y}$ (a) and $y(xx)\bar{y}$ (b) scattering geometries using the 514.5 nm excitation wavelength.

intensities of these two phonons decrease as the oxygen content decreases and two other disorder-induced modes clearly appear at 127.5 and $\sim$160 cm^{-1}. Therefore, the low-frequency region of the spectra (from $\sim$70 to $\sim$200 cm^{-1}) has been fitted with four Lorentzians. A direct comparison

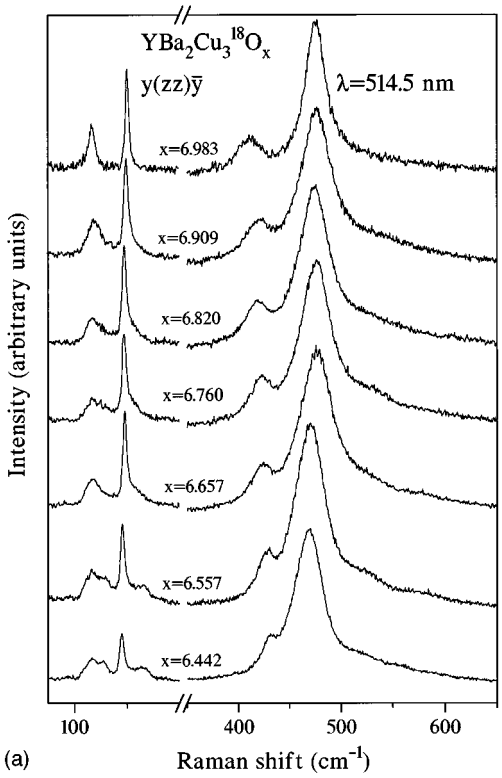

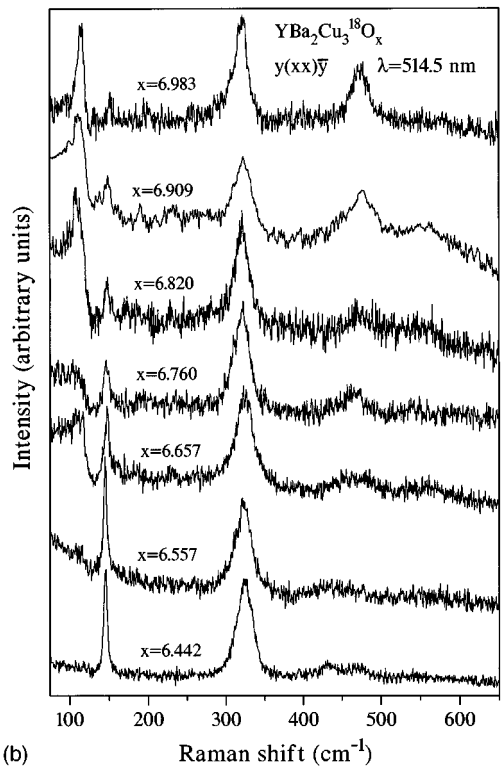

FIG. 2. Raman spectra for selected oxygen concentrations for the ^{18}O samples and for the $y(zz)\bar{y}$ (a) and $y(xx)\bar{y}$ (b) scattering geometries using the 514.5 nm excitation wavelength.

between the spectrum of $x=6.984$ sample and the spectrum of the $x=6.438$ sample where the splitting between the Ba and the 127.5 cm^{-1} peaks is apparent [Figs. 1(a) and 2(a)] shows that the Ba mode does not change with x. On the other hand, the Cu2 phonon frequency shows a slight linear increase from 144 cm^{-1} for $x=6.438$ to 150 cm^{-1} for $x=6.984$. From Figs. 1(a) and 2(a) it is apparent that the linewidth of the Cu2 peak remains small ($\sim$4 cm^{-1}) with an increase of 2 cm^{-1} with decreasing x and it is the same for both isotopes. In the xx polarization configuration [Figs. 1(b) and 2(b)] the asymmetry of the Ba line gradually increases

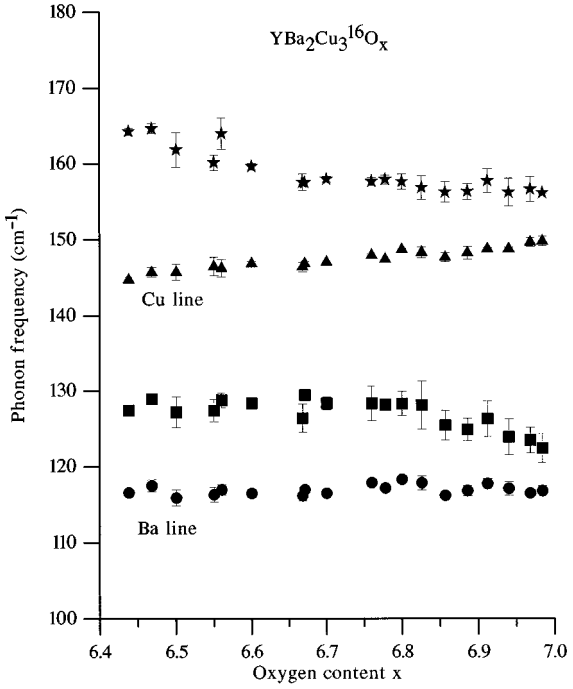

FIG. 3. Frequency shifts of the low-frequency Ba (●), Cu2 (▲), and two disorder-induced modes (⋆ and ■) for the ^{16}O samples as a function of the oxygen concentration.

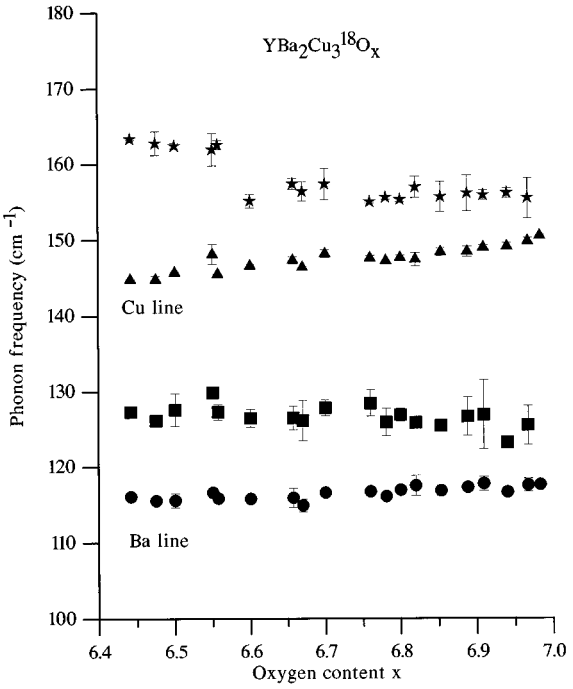

FIG. 4. Frequency shifts of the low-frequency Ba (●), Cu2 (▲), and two disorder-induced modes (⋆ and ■) for the ^{18}O samples as a function of the oxygen concentration.

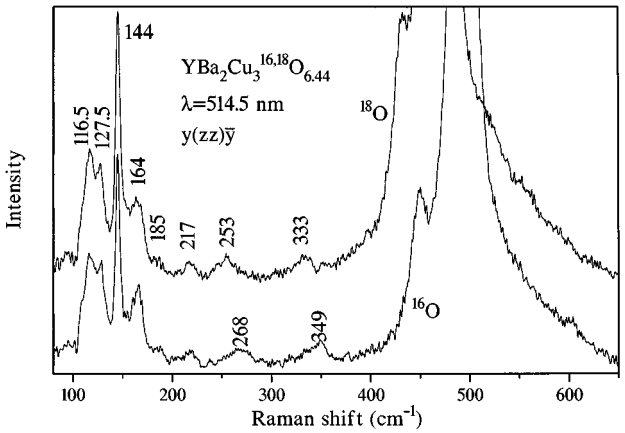

FIG. 5. Raman spectra for the $x=6.438$ (^{16}O) and 6.442 (^{18}O) samples obtained with the 514.5 nm excitation wavelength, in the $y(zz)\bar{y}$ scattering geometry.

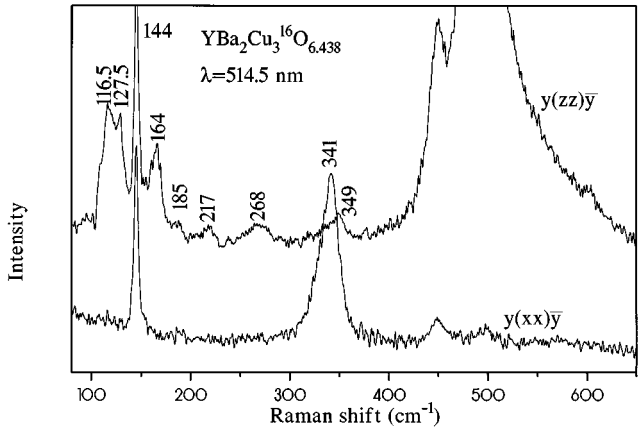

FIG. 6. Raman spectra for the $x=6.438$ and the ^{16}O isotope in the $y(zz)\bar{y}$ and $y(xx)\bar{y}$ scattering geometries, obtained with the 514.5 nm excitation wavelength.

while its intensity is reduced as x decreases and finally disappears near $x=6.50$. Inversely, the intensity of the Cu2 mode being negligible for $x=6.984$ gains about 1 order of magnitude for $x<6.50$. From the disorder-induced modes, the one at 127.5 cm^{-1} remains constant in frequency, while the other varies from 156 ($x=6.9$) to 164 cm^{-1} ($x=6.438$) as presented in Fig. 3.

Figure 5 shows the spectra for the $x=6.438$ (^{16}O) and $x=6.442$ (^{18}O) samples, where the Ba mode at 116.5 cm^{-1}, and the Cu2 at 144 cm^{-1}, remain at the same frequency for the two isotopes. The additional modes at 127.5, 164, 185, and 217 cm^{-1} are not affected by the isotopic substitution and can be unambiguously attributed to cation vibrations, contrary to Ref. 15 which attribute the 217 cm^{-1} peak to a defect-induced oxygen mode. Moreover, the 127.5 and 164 cm^{-1} peaks are somehow peculiar as they appear as high-frequency tails to the Ba and Cu2 peaks, respectively, even at high oxygen concentrations ($x\sim6.9$), while all other modes appear only in the $x=6.50$ region [see Figs. 1(a) or 2(b)]. The remaining of the peaks in Fig. 5, namely at 268 cm^{-1} (253 cm^{-1}) and 349 cm^{-1} (333 cm^{-1}), for ^{16}O (^{18}O), including the broad peak that has appeared at about 555 cm^{-1} (520 cm^{-1}) in the apex oxygen band fitting, clearly comes from oxygen vibrations, as it follows a harmonic behavior with its frequency being inversely proportional to the square root of the isotopic mass. One could roughly divide the YBCO phonon spectrum into the low-frequency cation vibration region, which extends up to about 220 cm^{-1} and the high-frequency oxygen region, which seems to have its lower end at about 260 cm^{-1}. In Fig. 6 the spectra for the ^{16}O sample with $x=6.438$ of Fig. 5 are shown in the zz and xx polarization geometries. With the possible exception of the peak at 349 cm^{-1}, which might be ''hidden'' into the strong B_{1g} band at 341 cm^{-1} in xx polarization, all the other modes present definite selection rules with only the zz component. For the high-frequency mode at 555 cm^{-1} it should be noted that its frequency is obtained from a multiple fitting of the apex modes as explained in Ref. 13. Therefore, there is an uncertainty in the accurate determination of its position, but the similar fitting of the ^{18}O data consistently induces this mode shifted by an amount in rough agreement with the mass ratio of the two isotopes. We therefore conclude that this mode should correspond to vibrations of an oxygen atom, probably the oxygen of the chains, which is IR active and becomes Raman active by disorder.

V. ANHARMONICITY OF THE OXYGEN MODES

Figure 7 shows the frequencies of the oxygen modes (obtained with the 488.0 and 514.5 nm excitation lines) with varying oxygen concentration for ^{16}O and for ^{18}O calibrated according to the square root of their mass ratio. The amount of the ^{16}O substitution by ^{18}O was estimated to be around

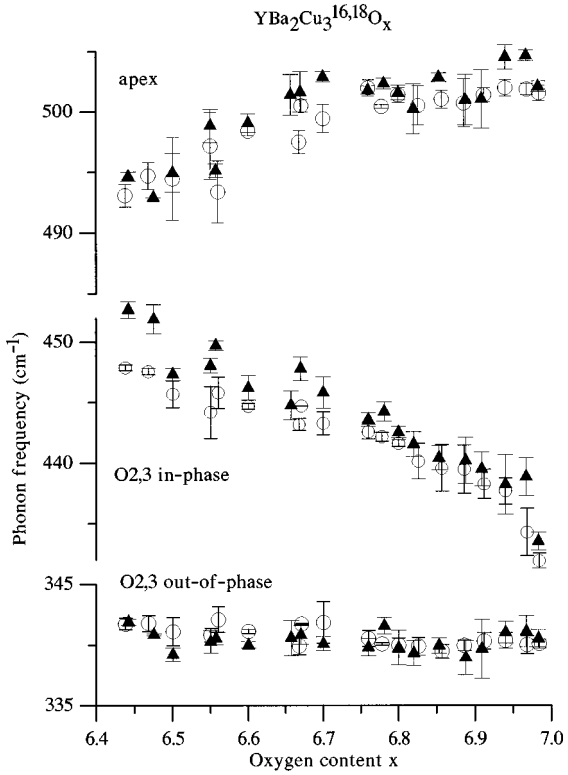

FIG. 7. The variation of the frequency of the oxygen modes with x for the ^{16}O (○) and the ^{18}O (▲, normalized according to the two isotopes average mass ratio and for 90% substitution), obtained with the 488.0 and the 514.5 nm excitation wavelengths.

85–90 % and is expected to be equally distributed at all oxygen sites.[8] Based on this amount one would expect a frequency shift of 5.5% (for 90% substitution) according to the average mass ratio of the two isotopes, or 5.3% with lattice dynamic calculations.[16] This difference, which for the apex oxygen phonon corresponds to 1 cm^{-1}, can be considered small compared with the statistical error in the Raman spectra (error bars) and the error in the correction factor (0.3%) which is related to the uncertainty on the amount of the isotopic substitution (5%). We have therefore used the simpler form of the mass ratio for the calculation of the theoretical isotope shift of the ^{18}O data and its comparison with the experimentally observed data of ^{16}O (Fig. 7). Theoretical calculations have shown that the oxygen isotope correction factor may slightly depend on the phonon modes[16] or on the oxygen concentration,[10] but here it was assumed constant, as the changes expected are minimal and any variation with the oxygen content will affect all modes in the same way.

For the out-of-phase oxygen mode (xx polarization) it can be seen that there is no anharmonic effect in the whole range of oxygen concentration in agreement with previous results.[9] The conclusion that the B_{1g} mode is not anharmonic will not be affected by the error in the estimated amount of oxygen isotope substitution (i.e., 85–90%), as the correction introduced in the phonon frequency (± 0.5 cm^{-1}) is small and within the experimental error. For the in-phase mode of the same oxygen atoms, there is a tendency for agreement of the ^{16}O and the ^{18}O (corrected) data at the optimum doping ($x \approx 6.92$) and in the overdoped region. It should be noted that the softening which has been discovered for $x \geqslant 6.92$ ^{16}O (Ref. 13) has the same behavior in the ^{18}O data (Fig. 7). For lower oxygen contents, the deviation from harmonicity for the in-phase mode increases with decreasing x. A similar behavior is observed for the apex oxygen, which shows no anharmonicity (or very small) in the optimally doped region, but there is an increasing deviation from harmonic behavior with decreasing x, though this deviation is not so systematic as in the case of the in-phase oxygen mode.

The above results seem to disagree with those of Ref. 9 concerning the apex oxygen (in that work the in-phase mode could not be studied). This difference could be attributed to the different excitation wavelength used in Ref. 9. Our recent work[13] has shown the existence of three phases contributing to the apex mode, and a resonance behavior for the phases of the apex mode has been established.[17] If we therefore assume that not all of the phases are anharmonic and definitely not the ortho-I, which is dominant for the optimally doped samples, the deviation between our data and those of Ref. 9 can be explained. The excitation with IR will increase the relative intensity of the anharmonic phases which appear with decreasing oxygen concentration and therefore at the same time increase the anharmonicity compared to the 514.5 nm excitation line which tends to be in resonance with the ortho-I phase.[13] In that case, the very small anharmonicity which might be present in the apex mode (Fig. 7), will actually map the variations in the relative intensities of the three phases as were actually observed before in the ^{16}O samples[13] and shown also for ^{18}O in Fig. 8. Another source for error is the site-selective substitution of the oxygen atoms which could affect the oxygen isotope correction factors for each oxygen atomic site (apex and plane oxygens). Based on the

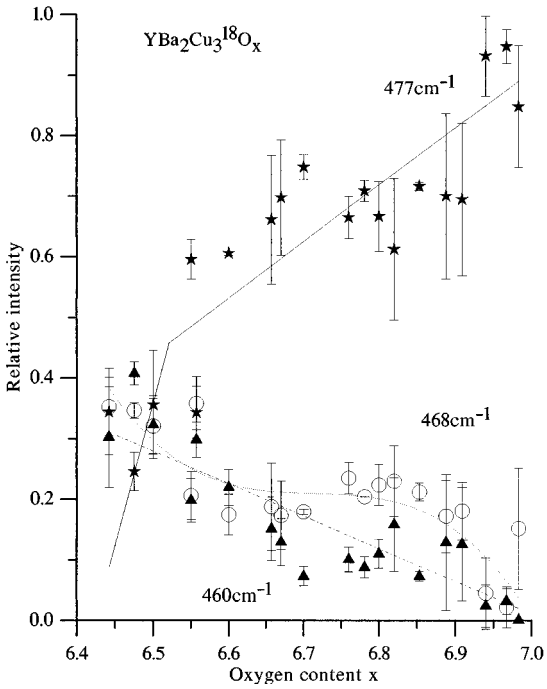

FIG. 8. The variation with oxygen concentration of the intensities of three phases of the apex phonon mode for ^{18}O, as obtained with multiple fitting (Ref. 13).

observation that the frequency of the B_{1g} mode does not vary with the amount of oxygen in both oxygen isotopes (Fig. 7), one could use the average values of the two frequencies for ^{16}O and ^{18}O in order to estimate the correction factor which turns out to be very close to the amount of ^{18}O substitution measured by other means ($\approx$90%). This indicates that there exists roughly the same amount of substitution in the apex and the plane oxygens.

To further reduce the consequences of a possible varying amount of substitution of ^{16}O for ^{18}O in different microcrystallites and samples on the phonon frequencies, as well as the possible dependence of the correction factor on the oxygen content,[10] we have divided the in-phase and apex mode frequencies by the corresponding out-of-phase frequency for each individual spectrum acquired. These ratios i.e., $\omega_{\text{in phase}}/\omega_{\text{out of phase}}$ and $\omega_{\text{apex}}/\omega_{\text{out of phase}}$ for both ^{16}O and ^{18}O are shown in Figs. 9 and 10 as a function of oxygen content. There appears to be a deviation from the harmonic behavior in the O2,3 in-phase vibrations for small values of oxygen content (Fig. 9) and to a smaller extent also for the apex mode (Fig. 10). To be more precise one should say that there is definitely a different behavior for the out-of-phase and the in-phase modes with decreasing amount of oxygen. For the apex mode the conclusions are the same as before, i.e., that close to optimum doping there is no anharmonicity (or a very small one), but there is a tendency for an increased (though smaller than in Ref. 9) anharmonicity with decreasing amount of oxygen. For comparison, the data from Ref. 9 have also been included and the deviation between the total amount of anharmonicity as well as its oxygen concentration dependence is quite clear.

As we have described above, the question of anharmonicity for the apical phonon is complicated by the presence of additional phases (at least two,[13]). In order to check the ef-

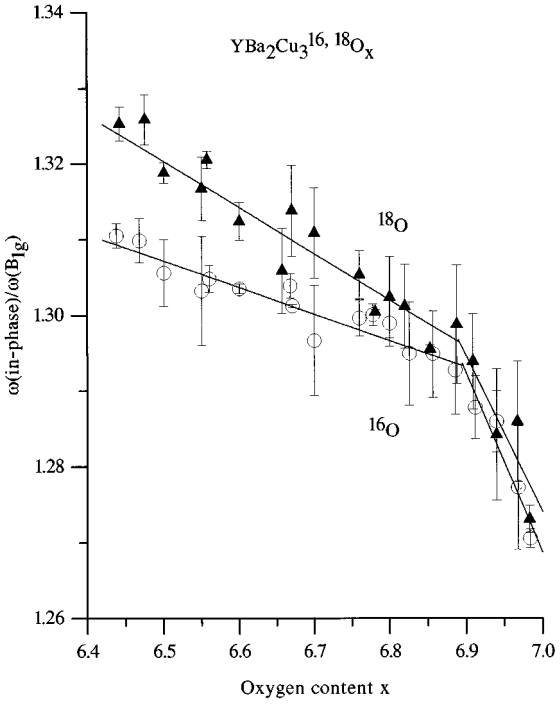

FIG. 9. The dependence on x of the ratio of the frequencies of the in-phase to the out-of-phase modes for ^{16}O (○) and ^{18}O (▲) obtained using the 488.0 and 514.5 nm excitation wavelengths. The straight lines are best linear fits to the corresponding portions of the data.

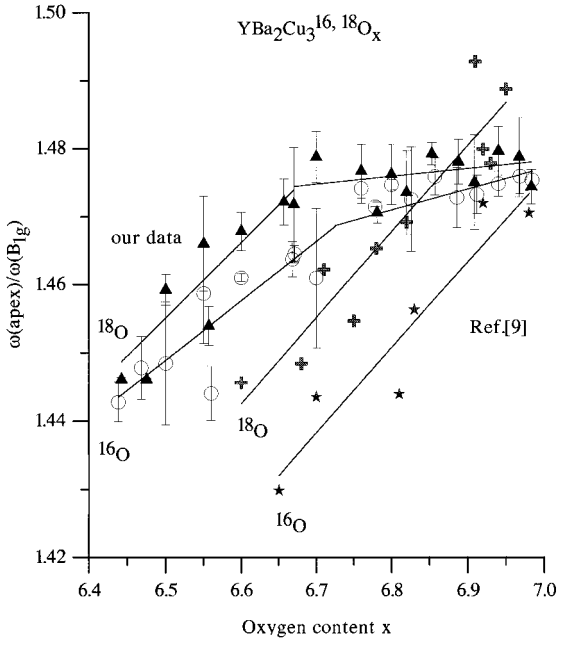

FIG. 10. The dependence on x of the ratio of the frequencies of the apex to the out-of-phase modes for ^{16}O (○) and ^{18}O (▲) and for the 488.0 and the 514.5 nm excitation wavelengths. The straight lines were drawn to guide the eye, according to the many-phases scheme discussed in Ref. 13. With the symbols ⋆ and + the corresponding data from Ref. 9 are depicted, together with their linear best fits.

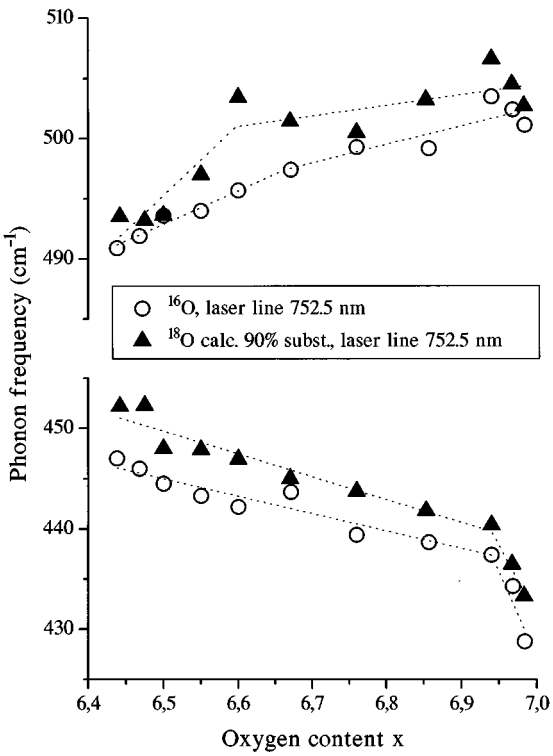

FIG. 11. The dependence of the frequencies of the apex and the in-phase modes on x for the ^{16}O (○) and ^{18}O (▲) using a 752.5 nm excitation wavelength. The straight lines are linear best fits to the corresponding portions of data.

fect of the excitation wavelength, we have used two more lines of the Kr^+ laser (647.1 and 752.5 nm) for probing. For the red line (647.1 nm) we have not observed any difference, while the results with the NIR line (752.5 nm) are shown in Fig. 11 for both the apex and the in-phase oxygen atoms. It can be seen that there is an increased error, as the very long accumulation times could not allow the study of many microcrystallites for better statistics, and of the B_{1g} mode for reference frequency as in Figs. 9 and 10. Apart from that, the conclusions for the apex oxygen are the same as with the other excitation wavelengths. In Ref. 9 an IR line has been used for excitation (at 1.1 eV compared with 1.55 eV for our wavelength). This difference in energy may be of importance for the anharmonicity of the apical mode, in case there is a resonance condition for one of the apex phases at this low excitation energy. Our present data however, do not seem to support any strong dependence of the apex oxygen anharmonicity on the excitation energy in the range of wavelengths studied. On the other hand, the anharmonic behavior of the in-phase phonon is reproduced even with the near IR line, being slightly larger for oxygen contents close to the optimum. This possible small dependence for the in-phase mode on the excitation wavelength (Fig. 11) will require a much better statistics in order to be verified. At this point we cannot really decide if the observed anharmonicity of the in-phase phonon should be related with the property of superconductivity, but its role should be examined in more detail as this phonon has also shown the characteristic softening beyond optimum doping in both oxygen isotopes (Figs. 7 and 11). The structural aspects of this effect are discussed in another publication.[18]

VI. SUMMARY

In conclusion our data show no anharmonicity for the O2,3 out-of-phase oxygen mode and this seems to be so in the whole range of oxygen concentrations studied. In contrast, an anharmonic behavior is observed for the O2,3 in-phase mode which depends strongly on the amount of oxygen. For the apical oxygen the problem is more complicated due to the existence of many contributing phases which appear to have a different amount of anharmonicity, with the ortho-I phase being harmonic in all excitation lines studied.

ACKNOWLEDGMENTS

E.K. acknowledges with appreciation the financial support of the Swiss National Fonds (NFP 30), which enabled the investigation in Zurich and D.P. acknowledges the support of the State Scholarships Foundation (I.K.Y.) of Greece.

[1] K. A. Müller, Z. Phys. B **80**, 193 (1990).
[2] R. E. Cohen, W. E. Pickett, and H. Krakauer, Phys. Rev. Lett. **64**, 2575 (1990).
[3] N. M. Plakida, V. L. Aksenov, and S. L. Drechsler, Europhys. Lett. **4**, 1309 (1987).
[4] T. Galbaatar, S. L. Drechsler, N. M. Plakida, and G. M. Vujici'c, Physica C **176**, 496 (1991).
[5] V. H. Crespi and M. L. Cohen, Phys. Rev. B **48**, 398 (1993).
[6] G. Ruani, R. Zamboni, C. Taliani, V. N. Denison, V. M. Burlakov, and A. G. Mal'shukov, Physica C **185-189**, 963 (1991).
[7] J. Mustre de Leon, S. D. Conradson, I Batistic, and A. R. Bishop, Phys. Rev. Lett. **65**, 1675 (1990).
[8] K. Conder, E. Kaldis, M. Maciejewski, K. A. Müller, and E. F. Steigmeier, Physica C **210**, 282 (1993).
[9] G. Ruani, C. Taliani, M. Muccini, K. Conder, E. Kaldis, H. Keller, D. Zech, and K. A. Müller, Physica C **226**, 101 (1994).
[10] E. Altendorf, J. Chrzanowski, J. C. Irwin, and J. P. Franck, Phys. Rev. B **43**, 2771 (1991).
[11] D. Mihailovic and C. M. Foster, Solid State Commun. **74**, 753 (1990).
[12] D. Mihailovic, K. F. McCarty, and D. S. Ginley, Phys. Rev. B **47**, 8910 (1993).
[13] N. Poulakis, D. Palles, E. Liarokapis, K. Conder, E. Kaldis, and K. A. Müller, Phys. Rev. B **53**, 534R (1996).
[14] K. Conder, S. Rusiecki, and E. Kaldis, Mater. Res. Bull **24**, 581 (1989).
[15] O. V. Misochko, S. Tajima, S. Miyamoto, and N. Koshizuka, Solid State Commun. **92**, 877 (1994).
[16] M. Cardona, R. Liu, C. Thomsen, W. Kress, E. Schonherr, M. Bauer, L. Gentzel, and W. Konig, Solid State Commun. **67**, 789 (1988).
[17] M. Iliev, C. Thomsen, V. Hadjiev, and M. Cardona, Phys. Rev. B **47**, 12 341 (1993).
[18] E. Kaldis, K. Conder, C. Krüger, E. Liarokapis, N. Poulakis, D. Palles, and K. A. Müller (unpublished).